Acta Crystallographica Section F
Structural Biology and Crystallization Communications
ISSN 1744-3091

ADP–Mg^{2+} bound to the ATP-grasp domain of ATP-citrate lyase

Tianjun Sun,‡ Koto Hayakawa and Marie E. Fraser*

Department of Biological Sciences, University of Calgary, 2500 University Drive NW, Calgary, AB T2N 1N4, Canada

‡ Current address: Department of Biochemistry, Queen's University, Kingston, ON K7L 3N6, Canada.

Correspondence e-mail: frasm@ucalgary.ca

Received 26 May 2011
Accepted 15 July 2011

PDB Reference: ATP-citrate lyase, 3pff.

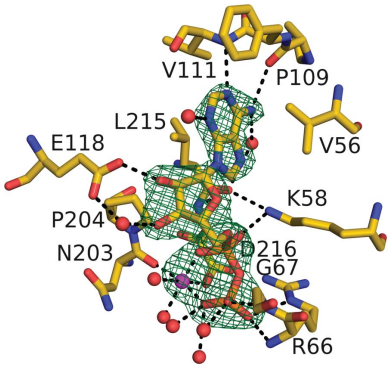

Human ATP-citrate lyase (EC 2.3.3.8) is the cytoplasmic enzyme that catalyzes the production of acetyl-CoA from citrate, CoA and ATP. The amino-terminal portion of the enzyme, containing residues 1–817, was crystallized in the presence of tartrate, ATP and magnesium ions. The crystals diffracted to 2.3 Å resolution. The structure shows ADP–Mg^{2+} bound to the domain that possesses the ATP-grasp fold. The structure demonstrates that this crystal form could be used to investigate the structures of complexes with inhibitors of ATP-citrate lyase that bind at either the citrate- or ATP-binding site.

1. Introduction

ATP-citrate lyase (ACLY) is the cytoplasmic enzyme in humans that links energy metabolism from carbohydrates to the production of fatty acids. Acetyl-CoA produced in the mitochondria cannot be exported to the cytoplasm. Instead, acetyl-CoA in mitochondria is transformed to citrate by citrate synthase and citrate is exported to the cytoplasm, where ACLY regenerates acetyl-CoA. The reaction catalyzed by ACLY is

$$\text{citrate} + \text{ATP} \rightarrow \text{acetyl-CoA} + \text{oxaloacetate} + \text{ADP} + \text{P}_\text{i}$$

and requires magnesium ions (Srere & Lipmann, 1953). Since ACLY is an enzyme upstream of the production of both cholesterol and fatty acids, it has been suggested as a drug target in the treatment of excess cholesterol and fat (Groot *et al.*, 2003). It has also been suggested as a drug target for the treatment of cancer: cancer cells have increased glycolysis and require *de novo* lipogenesis, metabolic processes that are linked by ATP-citrate lyase (Mashima *et al.*, 2009).

ACLY was discovered in pigeon liver (Srere & Lipmann, 1953), but many of the classical biochemical experiments were performed using the enzyme from rat liver. By forcing rats to fast and then feeding them a high-carbohydrate low-fat diet, the production of ACLY could be increased tenfold (Inoue *et al.*, 1965). Human and rat liver ACLY are 98% identical (Altschul *et al.*, 1997; Elshourbagy *et al.*, 1990, 1992; Groot *et al.*, 2003), so interpretations based on experiments with rat liver ACLY generally apply to the human enzyme as well. The enzyme is a homotetramer (Singh *et al.*, 1976), with each polypeptide chain containing 1101 amino-acid residues (Elshourbagy *et al.*, 1990)[1]. Apparent K_m values for the substrates citrate and ATP are 0.58 and 0.172 m*M*, respectively, at the optimal pH of 8.4 (Inoue *et al.*, 1966). Inoue and coworkers demonstrated that ACLY could be crystallized (Inoue *et al.*, 1965), although this experiment has been difficult to reproduce (Plowman & Cleland, 1967).

ACLY is a member of the superfamily of acyl-CoA synthetases (ADP-forming) (Sánchez *et al.*, 2000). The prototype for this family is succinyl-CoA synthetase, which catalyzes the formation of succinyl-CoA from succinate and CoA using ATP (Kaufman *et al.*, 1953). ACLY shows similarity to succinyl-CoA synthetase in its amino-terminal portion (Elshourbagy *et al.*, 1990) and this portion is thought to catalyze the formation of citryl-CoA in the same way that succinyl-CoA synthetase catalyzes the formation of succinyl-CoA (Wells, 1991). Both enzymes have an active-site histidine residue, which is

[1] The sequence presented in this paper had only 1100 amino-acid residues owing to errors in the sequencing.

Table 1
Statistics of the data collection.

Values in parentheses are for the outer shell.

Space group	*C*2
Unit-cell parameters (Å, °)	a = 167.54, b = 61.70, c = 107.98, α = 90, β = 125.5, γ = 90
No. of molecules in unit cell, Z	4
Matthews coefficient, V_M (Å^3 Da^{-1})	2.50
Solvent content (%)	51
Wavelength (Å)	0.9795
Temperature (K)	100
Resolution range (Å)	43.97–2.30 (2.42–2.30)
No. of unique reflections	39343
No. of measurements	150453
Completeness (%)	97.9 (92.82)
Multiplicity	3.8 (3.8)
$\langle I/\sigma(I)\rangle$	11.7 (1.7)
R_{merge}	0.084 (0.44)

Table 2
Structure refinement and model validation.

Values in parentheses are for the outer shell.

Resolution range (Å)	43.97–2.30 (2.35–2.30)
σ cutoff	$F > 0.00\sigma(F)$
Completeness (%)	94 (75)
No. of reflections used in refinement	35585 (1798)
No. of reflections above σ cutoff in final cycle	37841 (1883)
Final overall R factor	0.171
Atomic displacement model	Isotropic
No. of atoms	
Protein	5688
ADP–Mg^{2+}	28
Mg^{2+}	1
Solvent	389
Average B factors (Å^2)	
Protein	31
ADP–Mg^{2+}	27
Mg^{2+}	51
Solvent	35
Flat bulk-solvent model	B_{sol} = 40.88, k_{sol} = 0.37
Final R_{work}	0.1677 (0.2120)
No. of reflections for R_{free}	2256 (85)
Final R_{free}	0.2275 (0.2554)
Ramachandran plot analysis (*PROCHECK*; Laskowski *et al.*, 1993)	
Most favoured regions (%)	90.6
Additionally allowed regions (%)	9.4
Generously allowed regions (%)	0
Disallowed regions (%)	0

phosphorylated during catalysis (Kreil & Boyer, 1964; Mårdh *et al.*, 1971; Mitchell *et al.*, 1964). It has been proposed that this histidine residue shuttles the phosphoryl group from the nucleotide-binding site to the site where CoA and, presumably, the organic acid bind (Fraser *et al.*, 1999). The sequence of the carboxy-terminal portion of ACLY shows similarity to citrate synthase and is thought to catalyze the reverse reaction to citrate synthase: the cleavage of citryl-CoA to acetyl-CoA and oxaloacetate. In addition to these domains, human ACLY contains a stretch of residues that includes two serine residues and one threonine residue, which can be phosphorylated by protein kinase A (Pierce *et al.*, 1981), protein kinase B (Berwick *et al.*, 2002) or glycogen synthase kinase 3 (Ramakrishna *et al.*, 1990). These residues may play a role in regulation of the enzyme. A second isoform of ACLY exists which is ten residues shorter in this region.

To gain a better understanding of catalysis by human ACLY, the full-length enzyme was cloned, overproduced and purified with a carboxy-terminal His tag (Sun *et al.*, 2010). A form truncated by chymotrypsin was crystallized and the structure was solved by X-ray crystallography of the selenomethionyl protein. Based on the structure, the plasmid was modified to include only the sequence encoding the 817 amino-terminal residues of the enzyme linked to the carboxy-terminal His tag. This amino-terminal portion of human ACLY includes the binding site for citrate, which was revealed in the structure of the chymotrypsin-cleaved protein, and the domain that possesses the ATP-grasp fold (Murzin, 1996) and is expected to bind nucleotide (Sun *et al.*, 2010). The amino-terminal protein has now been used to investigate the ATP-binding site by growing crystals of the protein in complex with nucleotide.

2. Materials and methods

The amino-terminal portion of human ACLY was produced and purified as described previously (Sun *et al.*, 2010). The protein includes the 817 amino-terminal residues of human ACLY followed by the sequence $AALEH_8$. For crystallization, protein purified by immobilized metal-ion affinity chromatography was concentrated to 10 mg ml^{-1} as measured using the Bradford assay (Bradford, 1976) and dialyzed overnight in buffer consisting of 10 m*M* Tris–HCl, 10 m*M* $MgCl_2$, 2%(*v*/*v*) glycerol, 10 m*M* sodium citrate, 20 m*M* β-mercaptoethanol and 1 m*M* benzamidine pH 7.5. The sample was flash-frozen in 20 µl aliquots in thin-walled PCR tubes (Deng *et al.*, 2004).

Crystals were grown at 294 K in hanging drops using vapour diffusion. 25 µl protein solution at a concentration of 10 mg ml^{-1} was mixed with 10 µl 10 m*M* Tris–HCl pH 9, 2.5 µl 0.5 *M* ATP and 12.5 µl 0.1 *M* $MgCl_2$ to form the complex with the nucleotide. Hanging drops were made by mixing 0.5 µl of this solution with 0.5 µl precipitant solution and were equilibrated against 1 ml precipitant solution. The precipitant solution that gave good crystals consisted of 12.5%(*w*/*v*) polyethylene glycol 3350, 125 m*M* sodium tartrate, 100 m*M* Tris–HCl pH 8.2.

Prior to being shipped to the synchrotron for collection of X-ray diffraction data, crystals were transferred to mother liquor containing 20%(*v*/*v*) glycerol and vitrified in a stream of nitrogen gas at 100 K. Diffraction data were collected on beamline 08ID-1 of the Canadian Light Source, Saskatoon, Saskatchewan using a MAR Mosaic MX300 CCD detector. The data were processed using the program *MOSFLM* (Leslie, 1992), as well as programs from the *CCP*4 package (Winn *et al.*, 2011). Statistics of the data collection are presented in Table 1. The crystal is isomorphous with crystals grown in the absence of ATP and magnesium ions. The model used to calculate the initial electron-density maps was that of truncated human ACLY with tartrate bound (Sun *et al.*, 2010), identified in the Protein Data Bank (Berman *et al.*, 2000) as PDB entry 3mwe. A common set of reflections was used for the test set. ADP–Mg^{2+} was fitted into the electron density and the model was refined using the program *PHENIX* (Adams *et al.*, 2010). After cycles of rebuilding using the programs *MolProbity* (Chen *et al.*, 2010) and *Coot* (Emsley & Cowtan, 2004) and refinement, the final model was analyzed using programs from the *CCP*4 package (Winn *et al.*, 2011) as well as *Coot* (Emsley & Cowtan, 2004), *SPDBV* (Guex & Peitsch, 1997; Jones *et al.*, 1991) and *O* (Jones *et al.*, 1991). Statistics for the refined model are presented in Table 2. The coordinates and structure factors have been submitted to the Protein Data Bank (Berman *et al.*, 2000), where they have been assigned the identifier 3pff.

3. Results and discussion

ADP–Mg^{2+} binds to the domain of human ACLY possessing the ATP-grasp fold. The adenine base forms hydrophobic interactions with the protein by inserting between Val56 and Leu215 (Fig. 1, Table 3). N1 and N6 of the base form hydrogen bonds to backbone

atoms of residues linking the two subdomains that form the ATP-grasp fold. N6 also hydrogen bonds to a water molecule that bridges to one of the carboxylate O atoms of Glu108 (not shown in Fig. 1) and to the carbonyl O atom of Leu215. The ribose moiety donates a hydrogen bond from the O2′ hydroxyl group to Glu118 and forms a second hydrogen bond from the O3′ hydroxyl group to a water molecule that bridges to both Glu118 and the amide N atom of Val140 (not shown in Fig. 1). The pyrophosphate moiety interacts *via* the magnesium ion with both the side chain of Asp216 and the carbonyl of Asn203. In addition, the α-phosphate accepts a hydrogen bond from Lys58, while the β-phosphate accepts hydrogen bonds from the amide N atom and NE of the guanidinium group of Arg66 and the amide N atom of Gly67.

The conformational change in the enzyme required for the binding of ADP–Mg^{2+} is minimal. Residues in common between the crystal structures of the amino-terminal portion of human ACLY with and without ADP–Mg^{2+} bound superpose with a root-mean-squared deviation of 0.36 Å based on 2942 backbone atoms. At the binding site for ADP–Mg^{2+}, there are only small changes in the side chains of Asp216 and Lys58 and in the configuration of bound water molecules.

Although the protein was crystallized in the presence of ATP and magnesium ions, ADP–Mg^{2+} was found in the crystals. There are three possible reasons for this. The first is that ATP was contaminated with ADP or hydrolyzed to ADP and phosphate, and the protein crystallized in complex with ADP–Mg^{2+} instead of with ATP–Mg^{2+} because the enzyme has a higher affinity for ADP than for ATP. The apparent K_m for ADP is 4.1 ± 1.9 μ*M* (Plowman & Cleland, 1967), while the apparent K_m for ATP is 172 μ*M* (Inoue *et al.*, 1966) or 284 ± 23 μ*M* (Plowman & Cleland, 1967). The second possibility is that the ATP-grasp fold possesses some ATPase activity. This has been shown for two D-Ala-D-Ala ligases which also use the ATP-grasp fold to bind ATP (Neuhaus, 1962; Kitamura *et al.*, 2009). The third possible reason is that the γ-phosphate of ATP was transferred to His760, the active-site histidine residue, and ADP–Mg^{2+} remained bound to the enzyme. This transfer is the first step of the catalytic reaction,

$$\text{ATP} + \text{E} \rightarrow \text{E-P} + \text{ADP} \quad (1)$$

$$\text{E-P} + \text{citrate} \rightarrow \text{E} \cdot \text{citryl-P} \quad (2)$$

$$\text{E} \cdot \text{citryl-P} + \text{CoA} \rightarrow \text{E} \cdot \text{citryl-CoA} + \text{P}_i \quad (3)$$

$$\text{E} \cdot \text{citryl-CoA} \rightarrow \text{E} + \text{acetyl-CoA} + \text{oxaloacetate}, \quad (4)$$

where E represents the enzyme and E-P is the phosphorylated enzyme. Although the protein that was crystallized included the phosphohistidine loop, there was no electron density for residues 752–766. The same was true for previous crystal structures in which full-length human ACLY had been truncated with the protease chymotrypsin (Sun *et al.*, 2010). The absence of electron density, even when chymotrypsin was not used in crystallization, supports the interpretation that the disulfide bond formed between Cys293 and Cys748 leads to disorder of the phosphohistidine loop, as opposed to the interpretation that the loop was cleaved. Although it might seem counterintuitive that an extra bond would lead to disorder, Cys748 is likely to shift to interact with Cys293, dislodging the phosphohistidine loop from its interactions with the rest of the protein and leading to disorder of these residues.

The ADP-binding site of human ACLY is similar to that of *Escherichia coli* succinyl-CoA synthetase. Fig. 2 shows the superposition of the two binding sites based on the C^{α} coordinates of the residues shown in Fig. 1 and the equivalent residues of *E. coli* succinyl-CoA synthetase. One notable distinction between the two proteins is that in the complex of the amino-terminal portion of human ACLY with ADP–Mg^{2+} four water molecules are buried between ADP–Mg^{2+} and the protein in the same region where *E. coli*

Table 3
Interactions between ADP–Mg^{2+} and protein, ion or water atoms.

Distances of less than 3.2 Å between an atom of ADP–Mg^{2+} and the relevant atom in a residue, the Mg^{2+} ion or a water molecule are included. The equivalent residue in *E. coli* succinyl-CoA synthetase is listed in the final column where applicable.

Atom of ADP–Mg^{2+}	Residue, Mg^{2+} ion or water molecule	Atom	Distance (Å)	Equivalent residue in *E. coli* succinyl-CoA synthetase
N1	Val111	N	2.9	Thr102β
N3	Water 1156	O	3.0	
N6	Pro109	O	3.0	Ala100β
	Water 1139	O	2.7	
O3′	Water 1140	O	2.7	
O2′	Glu118	OE2	2.5	Glu107β
O1A	Mg 831	Mg	2.1	
O2A	Lys58	NZ	2.6	Lys46β
O1B	Arg66	N	2.8	Arg54β
		NE	2.8	
O2B	Mg 831	Mg	2.2	
	Water 1155	O	2.5	
	Water 1189	O	3.0	
O3B	Gly67	N	2.7	Gly55β
	Water 899	O	2.7	
Mg^{2+}	Asn203	O	2.1	Asn199β
	Asp216	OD2	2.3	Asp213β
	Water 1144	O	2.4	
	Water 1168	O	2.3	

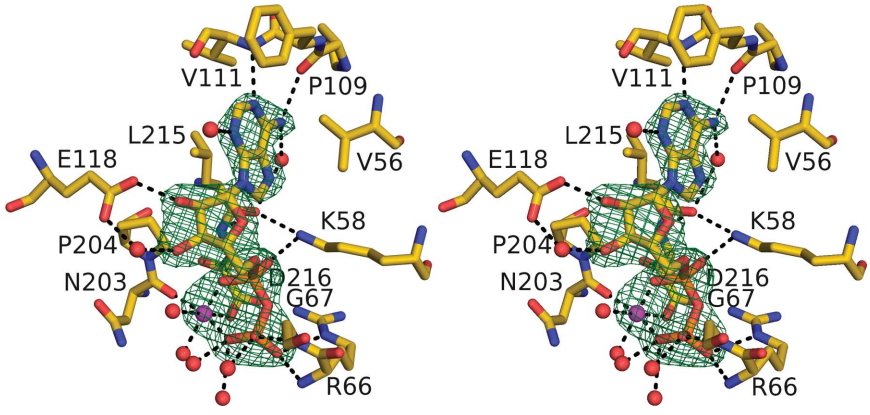

Figure 1
ADP–Mg^{2+}-binding site. In this stereofigure, residues with atoms within 3.4 Å of the ADP–Mg^{2+} are shown, as is Phe110 and the water molecules listed in Table 3. Dashed lines represent ionic interactions with Mg^{2+} or hydrogen bonds. The electron density, contoured at 4σ and shown in green, is from an $F_o - F_c$ OMIT map calculated after refinement when ADP–Mg^{2+} had been removed from the model. Figs. 1 and 2 were drawn using the program *PyMOL* (DeLano, 2002).

succinyl-CoA synthetase has a stretch of polypeptide that includes Pro20β (Fig. 2). These water molecules interact with each other and with Tyr16 of human ACLY. In pig GTP-specific succinyl-CoA synthetase, Gln20β, the residue equivalent to the proline, has been observed to interact directly with O6 of the guanine base and through a water molecule with N7, implicating this residue in the nucleotide-specificity of the enzyme (Fraser *et al.*, 2006). Comparison of GDP or GTP bound to GTP-specific succinyl-CoA synthetase with ADP bound to either *E. coli* succinyl-CoA synthetase or other enzymes that possess the ATP-grasp fold showed that the adenine base is located further into the binding pocket than the guanine base. While *E. coli* succinyl-CoA synthetase can bind either ADP/ATP or GDP/GTP (Murakami *et al.*, 1972), rat liver ACLY is specific for ADP/ATP (Inoue *et al.*, 1966). For GDP or GTP to bind, the guanine base would likely be held less deeply in the binding pocket than the adenine base. It would be expected to interact with the carbonyl O atom of Val111 through a hydrogen bond donated by N1 or N2. The specificity of ACLY for ATP is likely to be a function of several differences in the binding pocket for the base. First would be the absence of residues within the binding pocket that would be likely to interact with O6 of the guanine base. Secondly, the proline residue following Val111 would restrict the orientation of the carbonyl group of Val111, preventing optimal interaction of the carbonyl O atom with the guanine base. Thirdly, the large side chain of Phe110 where pig GTP-specific succinyl-CoA synthetase and *E. coli* succinyl-CoA synthetase have alanine residues could reduce the affinity for the guanine nucleotide because the guanine base would bind less deeply and displace the phenylalanine side chain.

The size, shape and properties of the nucleotide-binding pocket are relevant to the design of inhibitors targeting this site. Displacement of five water molecules, the one forming a hydrogen bond with N6 of adenine (Figs. 1 and 2) in addition to the four replacing the stretch of polypeptide in the binding pocket of succinyl-CoA synthetases (Fig. 2), adds depth to the pocket where adenine binds. In contrast to the ADP–Mg^{2+} complex with *E. coli* succinyl-CoA synthetase, ADP–Mg^{2+} appears to be more enclosed in the complex with the ATP-grasp domain of human ACLY. Lys66 from one side of the fold donates a hydrogen bond to Asp141 on the other side, and water molecules (not shown in Fig. 2) bridge the two sides across the β-phosphate. However, crystal packing may influence the conformations of these residues since a crystallographically related molecule interacts with both Lys66 and Asp141. Although it is clear from this structure that inhibitors that target the ATP-binding site and are about the same size as the nucleotide could crystallize in complex with the 817 amino-terminal residues of human ACLY in this crystal form, much larger inhibitors would be likely to disrupt the crystal packing.

4. Conclusions

The crystal structure of the 817 amino-terminal residues of human ACLY in complex with ADP–Mg^{2+} and tartrate has been determined at 2.3 Å resolution. Although the protein was crystallized in the presence of ATP and magnesium ions, ADP–Mg^{2+} rather than ATP–Mg^{2+} was seen in the complex. This may have been because the protein included the active-site histidine residue that is phosphorylated in the catalytic reaction and the γ-phosphoryl group could transfer from ATP–Mg^{2+} to form the phosphohistidine. The complex was crystallized in the presence of the inhibitor tartrate rather than the substrate citrate so that the phosphoryl group could not be transferred to the organic acid. However, the phosphohistidine may have been hydrolyzed because it was not protected by the parts of the protein with which it best interacts. Residues 752–766 of the phosphohistidine loop were not included in the model because there was no electron density for them. They may be disordered because the disulfide bond formed between Cys293 and Cys748 pulls Cys748 and hence the phosphohistidine loop out of position. The structure demonstrates that this crystal form could be used to investigate the

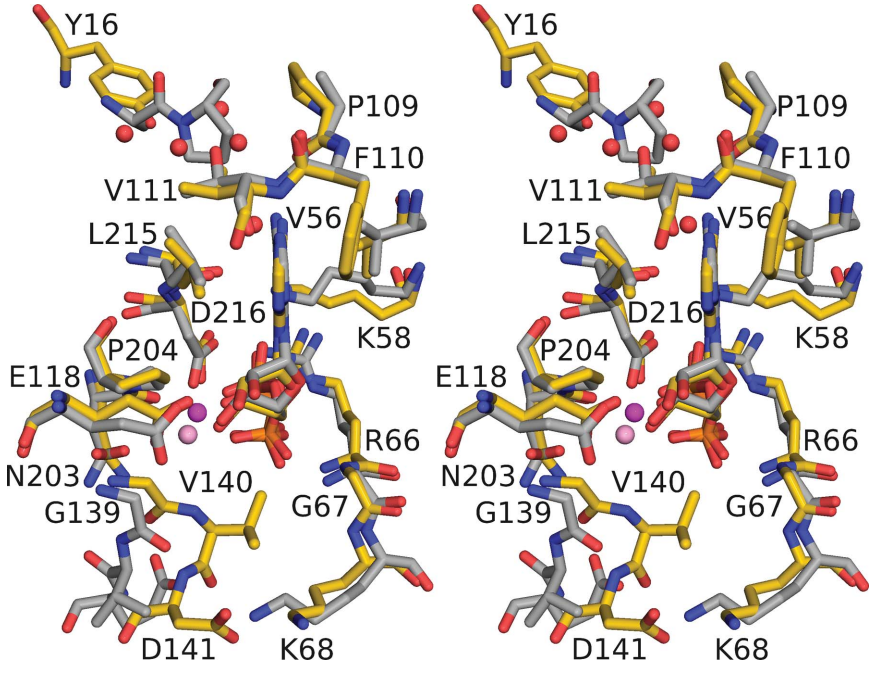

Figure 2
Comparison of the ADP-binding site of human ACLY with that of *E. coli* succinyl-CoA synthetase. To distinguish between the two complexes, the C atoms of human ACLY and ADP bound to it are coloured yellow, while those of *E. coli* succinyl-CoA synthetase and ADP bound to it are coloured grey in this stereofigure. The Mg^{2+} ions are shown in magenta when bound to ACLY and pink when bound to succinyl-CoA synthetase.

structures of complexes with inhibitors of ACLY that bind at either the citrate- or ATP-binding site.

Diffraction experiments described in this paper were performed at the Canadian Light Source, which is supported by the Natural Sciences and Engineering Research Council of Canada, the National Research Council Canada, the Canadian Institutes of Health Research, the Province of Saskatchewan, Western Economic Diversification Canada and the University of Saskatchewan.

References

Adams, P. D. *et al.* (2010). *Acta Cryst.* D**66**, 213–221.
Altschul, S. F., Madden, T. L., Schäffer, A. A., Zhang, J., Zhang, Z., Miller, W. & Lipman, D. J. (1997). *Nucleic Acids Res.* **25**, 3389–3402.
Berman, H. M., Westbrook, J., Feng, Z., Gilliland, G., Bhat, T. N., Weissig, H., Shindyalov, I. N. & Bourne, P. E. (2000). *Nucleic Acids Res.* **28**, 235–242.
Berwick, D. C., Hers, I., Heesom, K. J., Moule, S. K. & Tavare, J. M. (2002). *J. Biol. Chem.* **277**, 33895–33900.
Bradford, M. M. (1976). *Anal. Biochem.* **72**, 248–254.
Chen, V. B., Arendall, W. B., Headd, J. J., Keedy, D. A., Immormino, R. M., Kapral, G. J., Murray, L. W., Richardson, J. S. & Richardson, D. C. (2010). *Acta Cryst.* D**66**, 12–21.
DeLano, W. L. (2002). *PyMOL*. http://www.pymol.org.
Deng, J., Davies, D. R., Wisedchaisri, G., Wu, M., Hol, W. G. J. & Mehlin, C. (2004). *Acta Cryst.* D**60**, 203–204.
Elshourbagy, N. A., Near, J. C., Kmetz, P. J., Sathe, G. M., Southan, C., Strickler, J. E., Gross, M., Young, J. F., Wells, T. N. & Groot, P. H. (1990). *J. Biol. Chem.* **265**, 1430–1435.
Elshourbagy, N. A., Near, J. C., Kmetz, P. J., Wells, T. N., Groot, P. H., Saxty, B. A., Hughes, S. A., Franklin, M. & Gloger, I. S. (1992). *Eur. J. Biochem.* **204**, 491–499.
Emsley, P. & Cowtan, K. (2004). *Acta Cryst.* D**60**, 2126–2132.
Fraser, M. E., Hayakawa, K., Hume, M. S., Ryan, D. G. & Brownie, E. R. (2006). *J. Biol. Chem.* **281**, 11058–11065.
Fraser, M. E., James, M. N., Bridger, W. A. & Wolodko, W. T. (1999). *J. Mol. Biol.* **285**, 1633–1653.
Groot, P. H. E., Pearce, N. J. & Gribble, A. D. (2003). *Curr. Med. Chem. Immunol. Endocr. Metab. Agents*, **3**, 211–217.
Guex, N. & Peitsch, M. C. (1997). *Electrophoresis*, **18**, 2714–2723.
Inoue, H., Adachi, K., Suzuki, F., Fukunishi, K. & Takeda, Y. (1965). *Biochem. Biophys. Res. Commun.* **21**, 432–437.
Inoue, H., Suzuki, F., Fukunishi, K., Adachi, K. & Takeda, Y. (1966). *J. Biochem.* **60**, 543–555.
Jones, T. A., Zou, J.-Y., Cowan, S. W. & Kjeldgaard, M. (1991). *Acta Cryst.* A**47**, 110–119.
Kaufman, S., Gilvarg, C., Cori, O. & Ochoa, S. (1953). *J. Biol. Chem.* **203**, 869–888.
Kitamura, Y., Ebihara, A., Agari, Y., Shinkai, A., Hirotsu, K. & Kuramitsu, S. (2009). *Acta Cryst.* D**65**, 1098–1106.
Kreil, G. & Boyer, P. D. (1964). *Biochem. Biophys. Res. Commun.* **16**, 551–555.
Laskowski, R. A., MacArthur, M. W., Moss, D. S. & Thornton, J. M. (1993). *J. Appl. Cryst.* **26**, 283–291.
Leslie, A. G. W. (1992). *Jnt CCP4/ESF–EACBM Newsl. Protein Crystallogr.* **26**.
Mårdh, S., Ljungström, O., Högstedt, S. & Zetterqvist, O. (1971). *Biochim. Biophys. Acta*, **251**, 419–426.
Mashima, T., Seimiya, H. & Tsuruo, T. (2009). *Br. J. Cancer*, **100**, 1369–1372.
Mitchell, R. A., Butler, L. G. & Boyer, P. D. (1964). *Biochem. Biophys. Res. Commun.* **16**, 545–550.
Murakami, K., Mitchell, T. & Nishimura, J. S. (1972). *J. Biol. Chem.* **247**, 6247–6252.
Murzin, A. G. (1996). *Curr. Opin. Struct. Biol.* **6**, 386–394.
Neuhaus, F. C. (1962). *J. Biol. Chem.* **237**, 3128–3135.
Pierce, M. W., Palmer, J. L., Keutmann, H. T. & Avruch, J. (1981). *J. Biol. Chem.* **256**, 8867–8870.
Plowman, D. M. & Cleland, W. W. (1967). *J. Biol. Chem.* **242**, 4239–4247.
Ramakrishna, S., D'Angelo, G. & Benjamin, W. B. (1990). *Biochemistry*, **29**, 7617–7624.
Sánchez, L. B., Galperin, M. Y. & Müller, M. (2000). *J. Biol. Chem.* **275**, 5794–5803.
Singh, M., Richards, E. G., Mukherjee, A. & Srere, P. A. (1976). *J. Biol. Chem.* **251**, 5242–5250.
Srere, P. A. & Lipmann, F. (1953). *J. Am. Chem. Soc.* **75**, 4874.
Sun, T., Hayakawa, K., Bateman, K. S. & Fraser, M. E. (2010). *J. Biol. Chem.* **285**, 27418–27428.
Wells, T. N. (1991). *Eur. J. Biochem.* **199**, 163–168.
Winn, M. D. *et al.* (2011). *Acta Cryst.* D**67**, 235–242.